JOURNAL OF MATERIALS SCIENCE **33** (1998) 2519–2527

# Microstructural evolution of Al–Fe powder mixtures during high-energy ball milling

F. CARDELLINI*, V. CONTINI*‡, R. GUPTA§‖, G. MAZZONE*‡, A. MONTONE*, A. PERIN§, G. PRINCIPI§
** Ente Nazionale Energia Atterniva, Centro Ricerche Energia Casaccia, Settore Nuovi Materiali, C.P. 2400, 00100 Roma, Italy*
*‡ Istituto Nazionale per la Fisica della Materia, Unità di Perugia, Perugia, Italy*
*§ Istituto Nazionale per la Fisica della Materia, Dipartimento di Ingegneria Meccanica, Via Marzolo, 9, I-35131 Padova, Italy*
*E-mail: mazzone-g@casaccia.enea.it*

High-energy ball milling has been performed on $Fe_xAl_{1-x}$ powder mixtures with $x = 0.75$, 0.50, 0.25 and 0.20. X-ray diffraction, Mössbauer spectroscopy and electron microscopy have been used to characterize the samples milled for different times and annealed in a differential scanning calorimeter. It is found that, during milling, there is diffusion of both elements into each other, with a prevalence of iron diffusion into aluminium, at least in the early stages of the process. This behaviour is more pronounced in the aluminium-rich samples. The growth of the Fe(Al) and Al(Fe) solid solutions has been observed for $x \geqslant 0.5$, different from the lower iron concentrations where the Fe(Al) phase has not been detected. The annealing of pre-milled samples favours the formation, depending on the sample composition and on the annealing temperature, of intermetallic phases such as $Fe_3Al$, FeAl, $Fe_2Al_5$ and $FeAl_3$. © *1998 Chapman & Hall*

## 1. Introduction

The discovery that high-energy ball milling and extensive cold rolling of metallic systems are very effective means for inducing solid-state reactions at near room temperature has stimulated a lively debate on the microscopic mechanisms which are operative under these conditions.

In the case of high-energy ball milling of ductile components, the repeated process of forging, fracturing and cold welding leads to the formation of particles showing an irregularly convoluted multilayered structure which is progressively refined as milling proceeds [1]. Together with these microstructural changes, one observes the occurrence of a variety of solid-state reactions, such as alloying and nucleation of new phases, which require high atomic mobility and whose end products are, in many cases, in a metastable state. It has also been shown [2–4] that the phase transformations induced by extended milling are different from those observed after pre-milling followed by heat treatment. Therefore, the former reactions can hardly be a consequence of progressive refinement of the microstructure until the diffusion length at the effective process temperature becomes comparable with the average layer thickness. In summary, the microscopic phenomena which are at the origin of the solid-state reactions induced by extensive plastic deformation are not quite understood, particularly when these reactions take place at rates and in directions incompatible with a thermally activated mechanism [5].

Another interesting characteristic of mechanical alloying (MA) is its ability to produce relatively large amounts of materials with grain size $d \ll 1$ μm. Materials with such a small grain size are referred to as nanocrystalline materials and have been shown to have properties of great technological interest [6]. In particular, the nanocrystalline state improves the mechanical properties of intermetallic compounds by relieving, at least in part, the problems associated with their low room-temperature ductility. A considerable amount of work has therefore been concentrated on the synthesis by MA of transition-metal aluminides and in particular of iron aluminides. Restricting our attention to the more recent studies of these compounds [3, 4, 7–9], the end result of the milling process has been found to depend critically on the type of mill and on the milling conditions particularly in the Al-rich region [4]. Concerning the Fe-rich region (Fe concentration of 50 at% or greater) all studies have shown the formation of a body centred cubic (b.c.c.) solid solution whose X-ray diffraction (XRD) pattern shows very little, if any, B2 type of long-range order and none at all of the $D0_3$ type. The lattice parameter

---

‖ *Permanent address*: School of Instrumentation, Devi Ahilya University, Khandwa Road, Indore 452 001, India.

of this phase compared with that of pure α-Fe expands slightly upon milling notwithstanding a 15% difference between the atomic radii of Al and Fe. The measured expansion depends both on milling conditions and on composition being of the order of 2% at the 50 at % Fe concentration and 1.3% at the 75 at % Fe concentration under dry milling conditions [3] and about 1% at both concentrations under wet (ethanol) milling conditions [7]. It has also been observed [9] that the addition of ethanol slows down considerably the alloying reaction.

In all the experiments performed in the Fe-rich region, the first effect of milling is the progressive decrease and the final disappearance of the Al peaks in the XRD pattern, prior to the nucleation of any new phase. Rietveld analysis shows that most of this intensity decrease is not accompanied by a significant change in the lattice parameter of both Al and Fe [7]. It has also been found that the first phase nucleating upon heating of Fe-rich mixtures pre-milled for suitably short times is the intermetallic compound $Al_5Fe_2$, followed upon further heating by the formation of the B2 AlFe phase at the equiatomic composition and by a disordered Fe(Al) solid solution at 75 at% Fe [3, 7]. This finding establishes conclusively that, in agreement with literature data about diffusion coefficients reported in [3], Fe atoms diffuse into Al during thermally induced alloying.

The disappearance of the Al peaks mentioned above has been interpreted as an indication that, in the case of alloying induced by milling, the dominant mechanism is Al migration into Fe [7, 9]. In another study [3], mainly on the basis of indirect evidence, it has been deduced that Fe is the dominant moving species and that the prevailing microscopic mechanism at the origin of the alloying reaction is the dissolution of Fe into Al. In the same study the decrease in the Al intensity has been explained as due to a change in the effective absorption coefficient caused by a decrease in the particle size, as explicitly discussed in the case of Ni–Al [10] and W–C [11]. In fact the examination of ten binary systems containing equal atomic ratios of the component elements has shown a consistent trend that the heavier element persisted in the XRD spectra while the lighter element did not [12]. This phenomenon has been correctly attributed to refinement of the microstructure of the component elements even if absorption effects have not been explicitly mentioned.

In view of the conflicting opinions and of the lack of unequivocal experimental data concerning the course of the reactions occurring during ball milling of Al–Fe powder mixtures, we have performed a further study of these reactions using, in addition to XRD and differential scanning calorimetry (DSC), transmission electron microscopy (TEM) as a selective microanalytical tool and Mössbauer spectroscopy as an atomic level probe of the magnetic and structural state of the iron atoms.

## 2. Experimental procedure

Al powder of 99.95% purity (particle size, 50–100 μm) and Fe powder of 99.999% purity (particle size, 5–10 μm) both by Koch Chemicals were mixed in compositions with 25, 50, 75 and 80 at% Al. Milling of these mixtures was performed in steps of 30 min alternated with rest intervals of 5 min, using an air-cooled Spex 8000 mixer–mill equipped with a hardened steel vial and two steel balls of 13.5 mm diameter and 10 g mass (ball-to-powder ratio, 6 to 1). To prevent sample oxidation, the powders were sealed in the vial under an argon atmosphere and a fresh sample was used for each ball milling run. Morphological characterization of the milled particles was performed by scanning electron microscopy. TEM, Mössbauer spectroscopy and XRD were used for the microstructural characterization, while the thermal stability of the samples was tested by DSC. The Mössbauer data were recorded at room temperature by means of a standard spectrometer in transmission geometry using a $^{57}$Co source of about 3 mCi. The spectra were analysed with current least-squares minimization routines. The isomer shifts were referred to that of a metallic iron foil. XRD patterns were obtained using crystal focused and monochromated Co $K\alpha_1$ radiation in a Debye–Scherrer diffractometer equipped with a curved 120° position-sensitive detector. TEM observations were performed with a JEOL 4000 FX microscope equipped with an energy-dispersive spectroscopy (EDS) facility. The TEM samples were prepared by placing the powder between two Al foils 0.5 mm thick and then pressing the composite to a reduced total thickness of about 0.1 mm. The powder particles were thus embedded in the Al matrix from which small discs could be punched for further thinning by dimpling and for final polishing by Xe ion beam milling on a liquid-$N_2$-cooled stage. Thermal measurements from 100 to 700 °C were performed in a computer-assisted Perkin–Elmer DSC7 calorimeter operated in the specific heat mode at a constant heating rate of 0.25 $K\,s^{-1}$.

## 3. Experimental results

The Mössbauer spectra and the XRD patterns of the 75 at% Fe samples are shown in Figs 1 and 2, respectively. No appreciable variation with respect to pure α-Fe has been observed in the Mössbauer spectra of samples milled for 1 h or less in agreement with the invariance of the lattice spacings observed in the corresponding XRD patterns. Note that as reported in an earlier study [7] the invariance of the Mössbauer spectra and of the lattice spacings is accompanied by a marked decrease in the relative integrated intensity of the Al reflections. After milling for 2 h, the Mössbauer spectrum shows that in addition to the sharp sextet typical of α-Fe there is a doublet with a relative area (RA) of about 7% which marks the formation of a non-magnetic phase identified as a disordered solid solution containing Fe as the minority component. For longer milling times, in addition to the disappearance of the Al peaks there is also a progressive increase in the lattice spacings of the b.c.c. phase which, as previously reported [3], reaches a limiting value of about 1.3% after milling for 10 h. The presence of a second magnetic component represented by a broad sextet with a RA of about 50% is observed after

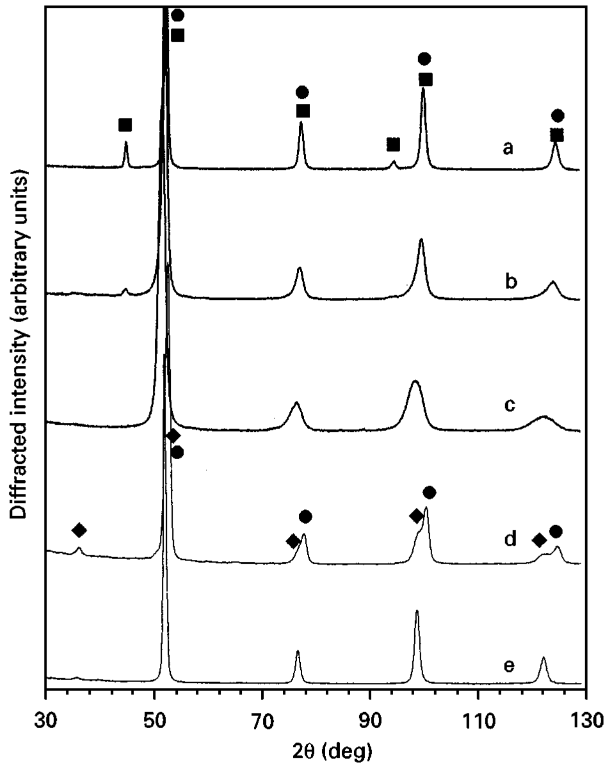

*Figure 1* XRD patterns of the 75 at% Fe samples, showing the Al (■), Fe(Al) (●) and FeAl (B2) (◆) peaks. Curve a, milled for 1 h; curve b, milled for 2 h; curve c, milled for 5 h; curve d, milled for 2 h and heated to 430 °C; curve e, milled for 2 h and heated to 700 °C.

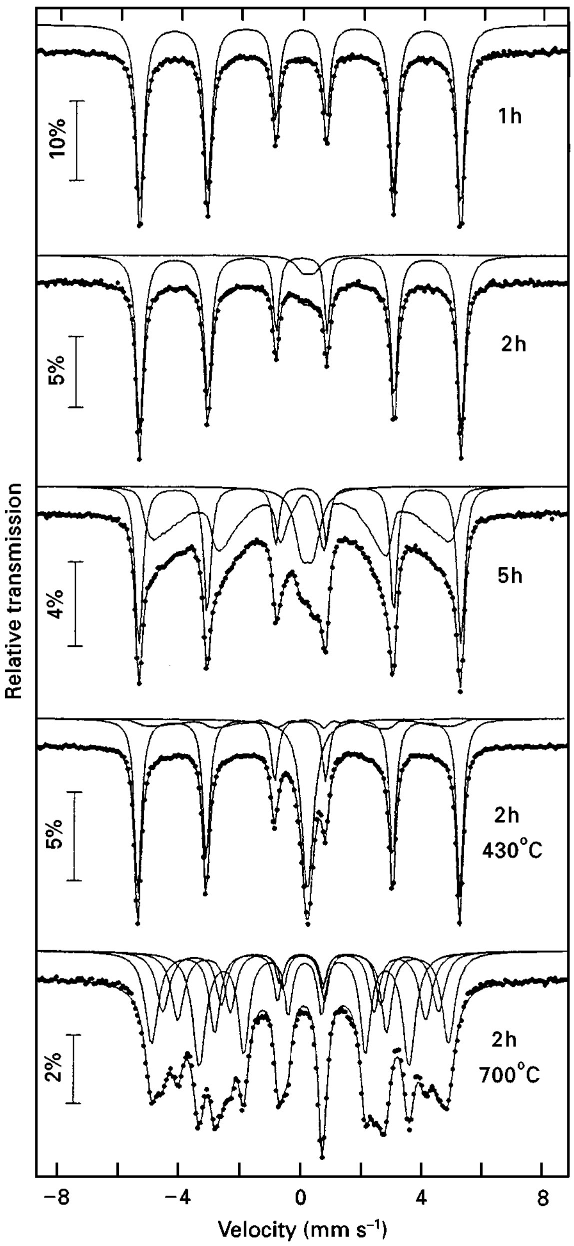

*Figure 2* Mössbauer spectra for the same samples as in Fig. 1.

TABLE I Computed hyperfine Mössbauer parameters of 2 h 25 at% Al–75 at% Fe sample after annealing to 700 °C: isomer shift δ; linewidth Γ (Γ which as been constrained to the same value for every sextet); hyperfine internal field $B_{hf}$; relative subspectral area RA; number $x$ of nearest-neighbour Al atoms according to [14]

| δ (mm s$^{-1}$) | Γ (mm s$^{-1}$) | $B_{hf}$ (T) | RA (%) | $x$ |
|---|---|---|---|---|
| 0.06 | 0.32 | 30.4 | 28 | 1 |
| 0.07 | 0.32 | 28.1 | 18 | 2 |
| 0.11 | 0.32 | 25.4 | 20 | 3 |
| 0.18 | 0.32 | 21.5 | 34 | 4 |

milling for 5 h. This component, according to its XRD pattern, can be identified as an Fe-rich solid solution with a b.c.c. structure. Heating of the 2 h sample to 430 °C causes the disappearance of the doublet, the decrease unreacted α-Fe to a RA of about 60%, the formation of a magnetic phase similar to that observed in the 5 h sample and, finally, the appearance of a strong singlet. This singlet, comparing its parameters with literature values [13], can be attributed to a defective FeAl B2 phase, in agreement with the same conclusion arrived at in an earlier paper on the basis of the XRD pattern [3]. The Mössbauer spectrum of the 2 h sample heated to 700 °C is very different. Its fitting requires four sextets with the parameters reported in Table I. According to Gao and Fultz [14], these sextets correspond to ferromagnetic Fe in different b.c.c. environments characterized by a number of Al nearest neighbours ranging from one to four. The information derived from the XRD pattern of this sample is much more limited, showing only the formation of an almost completely disordered b.c.c. solid solution. The Mössbauer data of all samples examined in the present study are collected in Table II.

The Mössbauer spectra and the XRD patterns of the equiatomic samples are shown in Figs 3 and 4, respectively. After milling for 3 h, one observes the presence of a doublet and of a broad sextet corresponding, as in the 75 at% Fe samples, to a disordered non-magnetic Al-rich and to a disordered magnetic Fe-rich solid solution. The spectrum of the 5 h sample shows, in addition to the components observed in the 3 h sample, a singlet ascribed to the FeAl B2 phase with structural defects as indicated by the relatively large linewidth. The RA of the sharp sextet decreases with increasing milling time from 3 to 10 h and this decrease is almost completely made up for by an increase in the RA of the singlet which, in the 10 h sample, is the main component. At this composition, both magnetic components disappear after milling for 30 h so that only the singlet and the doublet are observed. The same components, with different hyperfine parameters and RAs, are observed in the spectrum of the 10 h sample heated to 700 °C, in which the

TABLE II Computed hyperfine Mössbauer parameters of the analysed samples: isomer shift δ; linewidth Γ; quadrupole splitting Δ; average hyperfine internal field $\langle B_{hf} \rangle$; relative subspectral area RA.

| Sample | MA time (h) | Annealing temperature (°C) | Singlet | | | Doublet | | | | Broad sextet | | Sharp sextet |
|---|---|---|---|---|---|---|---|---|---|---|---|---|
| | | | δ (mm s$^{-1}$) | Γ (mm s$^{-1}$) | RA (%) | (δ) (mm s$^{-1}$) | Δ (mm s$^{-1}$) | Γ (mm s$^{-1}$) | RA (%) | $\langle B_{hf} \rangle$ (T) | RA (%) | RA (%) |
| $Fe_{75}Al_{25}$ | 1 | — | — | — | — | — | — | — | — | — | — | 100 |
| | 2 | — | — | — | — | 0.22 | 0.37 | 0.56 | 7 | — | — | 93 |
| | 5 | — | — | — | — | 0.22 | 0.37 | 0.56 | 12 | 25 | 52 | 36 |
| | 2 | 430 | 0.25 | 0.47 | 25 | — | — | — | — | 26 | 12 | 63 |
| | 2 | 700 | — | — | — | — | — | — | — | — | — | (see Table I) |
| $Fe_{50}Al_{50}$ | 3 | — | — | — | — | 0.22 | 0.45 | 0.47 | 17 | 26 | 34 | 49 |
| | 5 | — | 0.25 | 0.46 | 14 | 0.22 | 0.43 | 0.41 | 31 | 24 | 30 | 25 |
| | 10 | — | 0.25 | 0.47 | 34 | 0.21 | 0.40 | 0.39 | 30 | 20 | 28 | 8 |
| | 30 | — | 0.23 | 0.44 | 33 | 0.19 | 0.40 | 0.46 | 67 | — | — | — |
| | 10 | 700 | 0.26 | 0.28 | 58 | 0.22 | 0.29 | 0.28 | 42 | — | — | — |
| $Fe_{25}Al_{75}$ | 10 | — | — | — | — | 0.20 | 0.46 | 0.25 | 45 | — | — | 55 |
| | 20 | — | — | — | — | 0.24 | 0.50 | 0.40 | 89 | — | — | 11 |
| | 20 | 700 | — | — | — | 0.24 | 0.43 | 0.33 | 100 | — | — | — |
| $Fe_{20}Al_{80}$ | 20 | — | — | — | — | 0.19 | 0.44 | 0.38 | 66 | — | — | 34 |
| | 50 | — | — | — | — | 0.21 | 0.54 | 0.40 | 100 | — | — | — |
| | 20 | 700 | 0.22 | 0.26 | 35 | 0.21 | 0.39 | 0.24 | 65 | — | — | — |

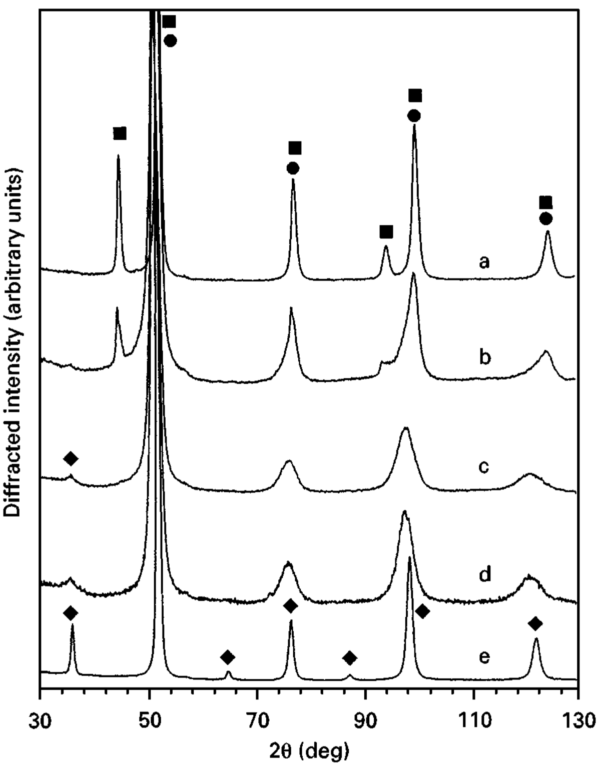

*Figure 3* XRD patterns of the equiatomic samples, showing the Al (■), Fe(Al) (●) and FeAl(B2) (◆) peaks. Curve a, milled for 3 h; curve b, milled for 5 h; curve c, milled for 10 h; curve d, milled for 30 h; curve e, milled for 10 h and heated to 700 °C.

sharp singlet of the FeAl B2 phase predominates. Particularly significant is the evolution of the hyperfine field distribution of the broad sextet displayed on the right-hand side of Fig. 4 which corresponds to an increase in the Al content in the disordered Fe-rich b.c.c. phase with increasing time of milling. The XRD patterns of these samples show the progressive decrease in the intensity of the Al peaks together with an increase in the lattice spacings of about 2%. A very weak (1 0 0) superstructural reflection is observed in the 10 h sample while the Mössbauer spectra, more sensitive to local order, show the formation of B2 nuclei already after milling for 5 h.

The Mössbauer spectra and the XRD patterns of the Al-rich samples are shown in Figs 5–8. At both compositions there is no appreciable growth of the broad sextet corresponding to the Fe-rich magnetic component. The main phase change corresponds to a decrease in the sharp sextet of α-Fe and to the growth of a doublet whose parameters at both compositions and for all milling times are similar to those reported for the $Al_5Fe_2$ compound [13]. For the 75 at% Al composition the doublet is observed with a RA of about 45% in the sample milled for 10 h, for which no evidence of the $Al_5Fe_2$ phase is found in the XRD pattern. This discrepancy, which has been checked repeating both the Mössbauer and the diffraction spectrum, can be explained by the higher sensitivity of Mössbauer spectroscopy to local arrangements as recalled above. The difficulty of interpreting XRD patterns arising from partially ordered structures is clearly evidenced by the 80 at% Al sample milled for 50 h whose local structure of the $Al_5Fe_2$ type can only be deduced from the Mössbauer spectrum. Good agreement between the Mössbauer and the X-ray results is observed in the samples heated to 700 °C which appear to be single-phase $Al_5Fe_2$ at 75 at% Al and single-phase $Al_3Fe$ at 80 at% Al.

The morphology of the powders is presented in Fig. 9 which shows three scanning electron micrographs at different milling times and compositions. At both the 75 and the 50 at% Fe concentrations the convoluted microstructure is observed to be well developed after milling for 2 h with a comparable degree of refinement of the lamellae. In contrast, the sample milled for 1 h appears to be much coarser and inhomogeneous. The same features appear on a finer scale on two transmission electron micrographs shown in Fig. 10. The TEM observations, performed

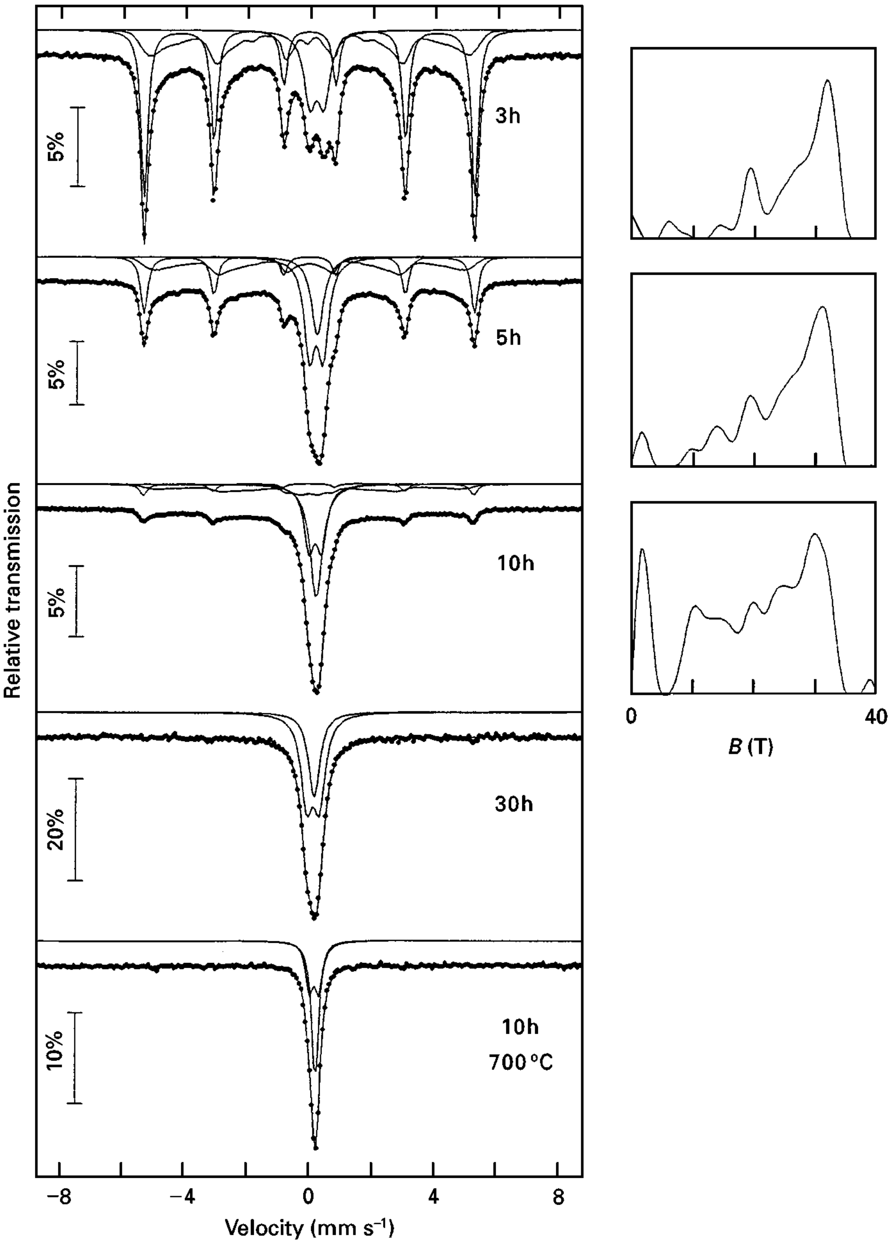

*Figure 4* Mössbauer spectra for the same samples as in Fig. 3. The hyperfine field distributions of the broad magnetic component are displayed on the right-hand side.

on an Fe-rich sample milled for 1 h and on an equiatomic sample milled for 2 h, were aimed at studying the early stages of the alloying process. In order to obtain significant analytical data, the multilayer was aligned as carefully as possible with the interfaces parallel to the electron beam. A small beam with a spot size of a few tens of nanometres was used to collect simultaneously the X-ray emission spectrum for chemical analysis and the electron diffraction pattern for phase analysis.

The equiatomic sample showed a lamellar structure with light and dark areas. The observed contrast did not change appreciably upon small variations in the angle between the electron beam and the normal to the sample surface, thus indicating the contrast variation to be of chemical origin rather than diffraction. This conclusion was confirmed by EDS analysis which showed systematically a much higher Fe content in the dark areas than in the light areas. The iron content was measured scanning the electron beam along a direction perpendicular to the interfaces and in the case of the dark areas was essentially constant inside each lamella. A limited variation, however, was observed in different lamellae, with the Fe content ranging between 90 and 100 at% in all measurements and being of the order of 98–99 at% in many cases. The measurements performed on the light areas gave very different results, showing a large variation in the Fe content inside each lamella and in different lamellae. The iron content ranged between 15 and 50 at% and in no case was it possible to find a spot consisting of only pure Al. No conclusive evidence was obtained from the microdiffraction patterns which in almost all cases consisted of more than one nanocrystalline grain. This fact coupled with the coincidence of the Fe lattice spacings with most of the Al spacings prevented a clear identification of the crystal structure of both areas. Microdiffraction patterns recorded placing

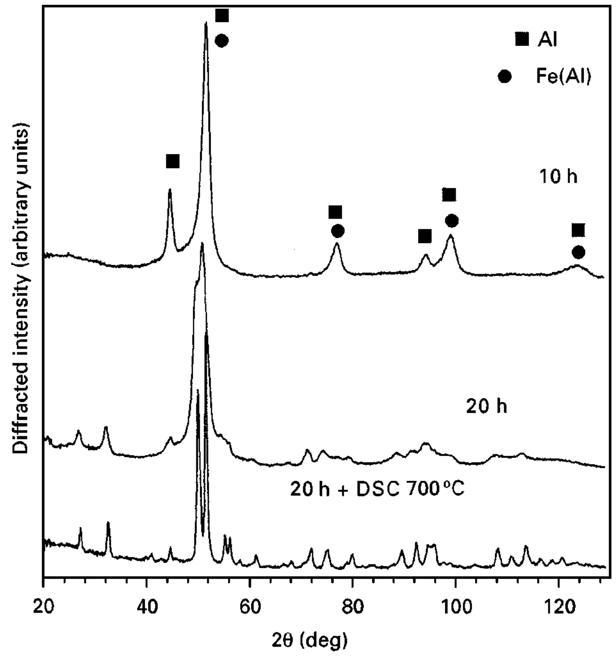

*Figure 5* XRD patterns of the 75 at% Al samples milled for different times and after heat treatment, showing the Al (■) and Fe(Al) (●) peaks.

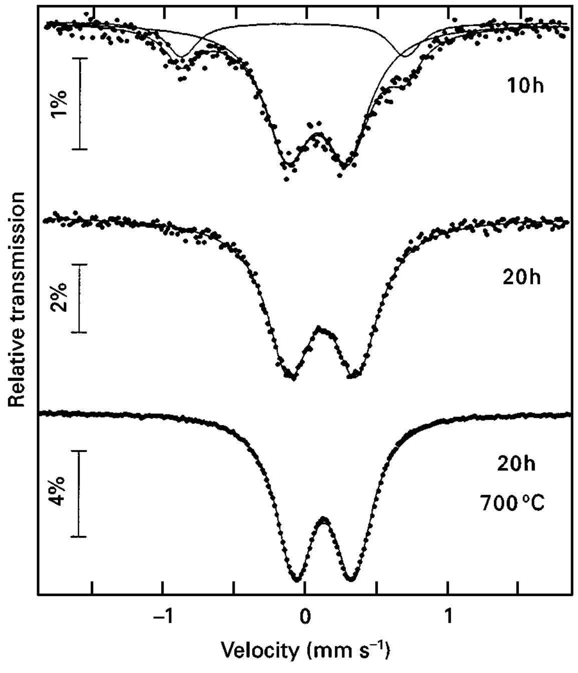

*Figure 6* Mössbauer spectra for the same samples as in Fig. 5. The weak outer doublet in the Mössbauer spectrum of the 10 h sample corresponds to the inner lines of the sharp sextet of unreacted iron.

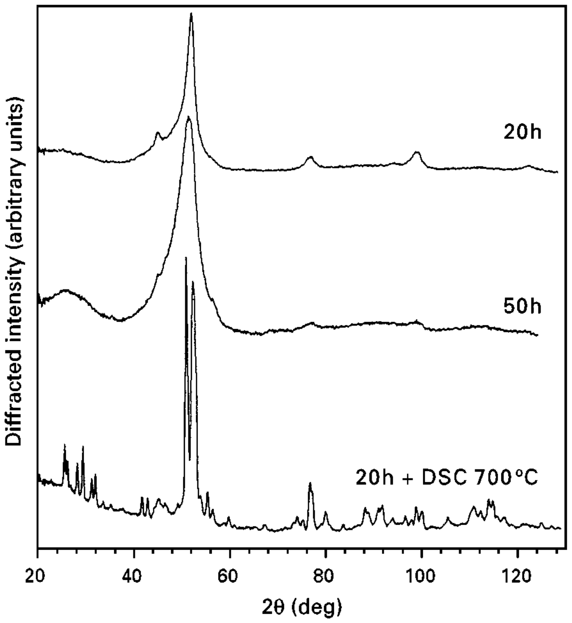

*Figure 7* XRD patterns of the 80 at% Al samples milled for different times and after heat treatment.

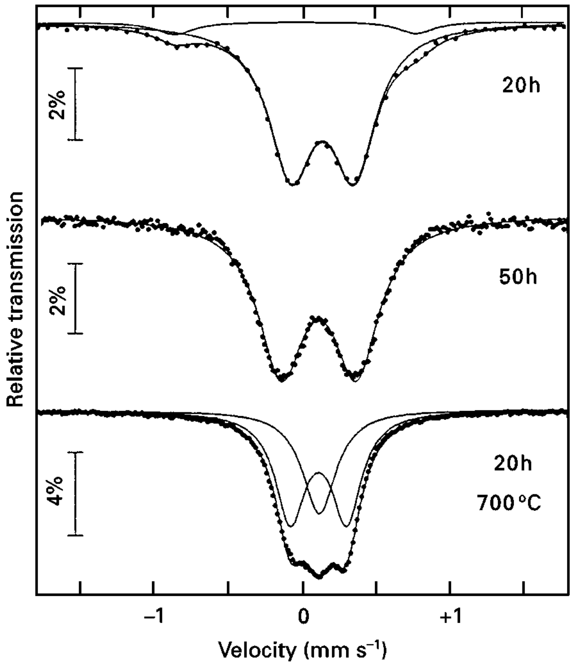

*Figure 8* Mössbauer spectra for the same samples as in Fig. 7. The weak outer doublet in the Mössbauer spectrum of the 20 h sample corresponds to the inner lines of the sharp sextet of unreacted iron.

the beam across an interface failed to reveal any of the intermetallic phases of the Al–Fe system.

The microstructure of the Fe-rich sample milled for 1 h is much less regular with only a few areas showing a lamellar structure on a fine scale. It was also much more difficult to align the lamellae along the electron beam so that both the analytical and the structural data may not refer to a single lamella. The Fe content of the dark areas ranged also in this sample between 90 and 100 at% with a majority of values close to 100 at%. The Fe content of the light areas, on the contrary, was even more variable than in the equiatomic sample. In many cases, one could observe in the corresponding microdiffraction pattern the (111) spot of Al with a lattice spacing of 0.23 nm, thus showing that the crystal structure of the light areas was totally or in part face-centred cubic. In the same areas, similar to the observations performed on the equiatomic sample, it was impossible to find a spot consisting of only pure Al whose concentration was never found to exceed approximately 80 at%.

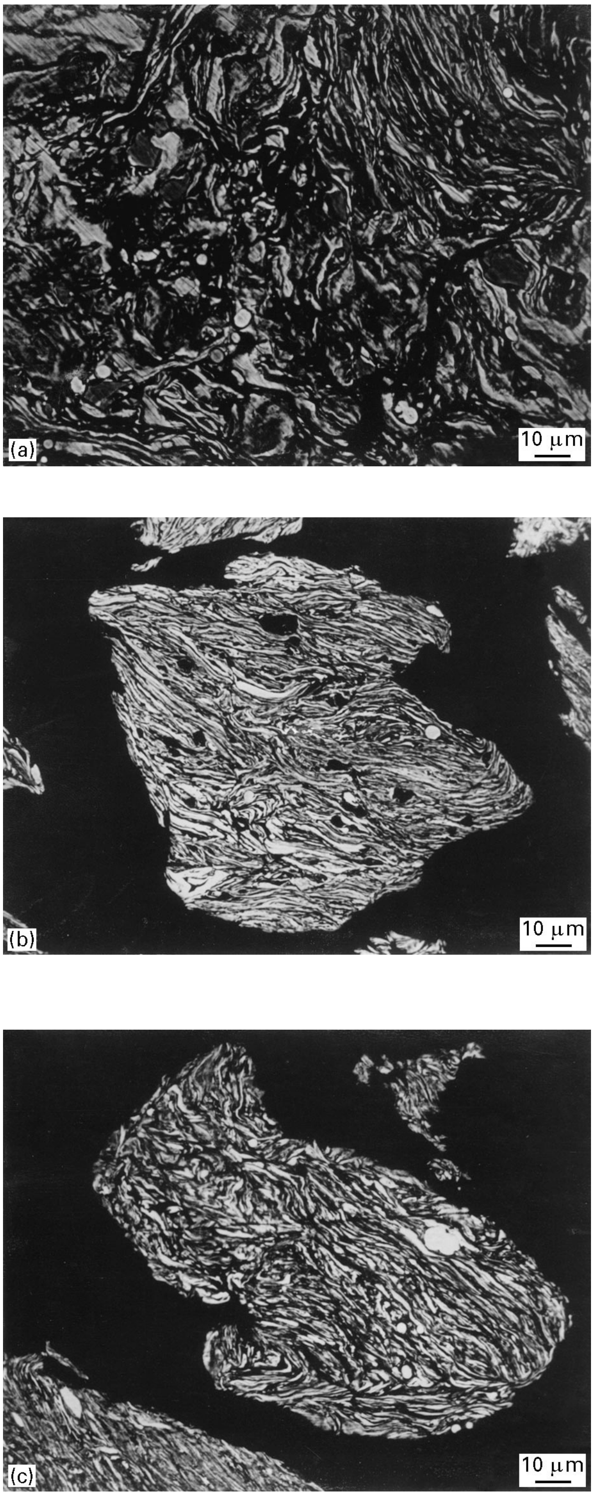

*Figure 9* Scanning electron micrographs of (a) 25 at% Al–75 at% Fe milled for 1 h, (b) 25 at% Al–75 at% Fe milled for 2 h and (c) 50 at% Al–50 at% Fe milled for 2 h.

## 4. Discussion

The results of the present study, coupled with those of previous investigations [3, 4], allow a fairly complete description of the phase transformations induced by high-energy ball milling of Al–Fe powders and the identification of the main microscopic mechanisms which influence the course of the observed solid-state reactions. In accordance with the conclusions reached in previous studies [3, 4, 10–12] the Mössbauer spectra and the scanning electron micrographs of the Fe-rich and of the equiatomic samples show that the change in the relative intensities observed in the XRD patterns recorded during the first stages of milling are due to a large extent to microstructural refinement. The alloying reaction proceeds at an appreciable rate after an incubation time (corresponding to the formation of a sufficiently refined multilayered structure) depending on composition and milling conditions. The influence of the Al concentration on the interdiffusion rate has already been mentioned in the introduction. In particular, a calorimetric study reported in Fig. 11, shows that, upon heating of the samples to 700 °C, there is no appreciable heat release in 75 at% Al–25 at% Fe samples milled for at least 20 h. The same feature is observed in the equiatomic samples milled for 10 h and, for the 75 at% Fe composition, in samples milled for only 5 h. Fig. 11 shows also that for the 80 at% Al composition there is still a substantial heat release upon heating of a sample milled for 50 h. Considering that the absence of a significant heat release during DSC heating is an indication that most of the interdiffusion process has already occurred during milling, the above calorimetric observations point to a considerable decrease in the rate of interdiffusion with increasing Al content, in agreement with the rate of change in the Mössbauer spectra observed in the present study. The Mössbauer spectra and the results of EDS microanalysis allow one also to assess the role played by Al and Fe atoms in the interdiffusion process. The first component which is observed to grow in the Mössbauer spectra of the Fe-rich samples is a non-magnetic phase with an Fe content below about 50 at% as a result of Fe diffusing into Al. Together with this component (according to [7]) or immediately after (according to the present experiment), one observes the growth of a magnetic component characterized by a broad hyperfine field distribution identified as an Fe-rich solid solution growing as a result of Al diffusion into Fe. The spectrum recorded after heating the 2 h sample to 430 °C (Fig. 1d) shows the formation of a cubic non-magnetic component, which can be ascribed to a defective AlFe B2 phase, as a result of further diffusion of Fe in the Al-rich phase, together with the appearance of the broad sextet of the Fe-rich phase. In summary, one has that diffusion of both elements is operative at this composition in both the thermally activated and the mechanically assisted conditions. A similar situation occurs at the equiatomic composition where one observes the growth of a non-magnetic phase as a result of Fe diffusing into Al and of a magnetic phase, whose Al content increases with milling time, as a result of Al diffusing into Fe. The same components have been observed also in the equiatomic samples of [7] with the formation of the magnetic phase delayed with respect to the non-magnetic phase. For longer milling times, the present samples show the formation of another non-magnetic component identified as a defective AlFe B2 phase, not observed in the Mössbauer spectra reported in [7] for samples milled up to 32 h with ethanol. An increase in the amount of the B2 phase is observed after heating to 700 °C the sample milled for 10 h in accordance with similar results reported in [7]. Notwithstanding considerable sharpening of the XRD patterns, the

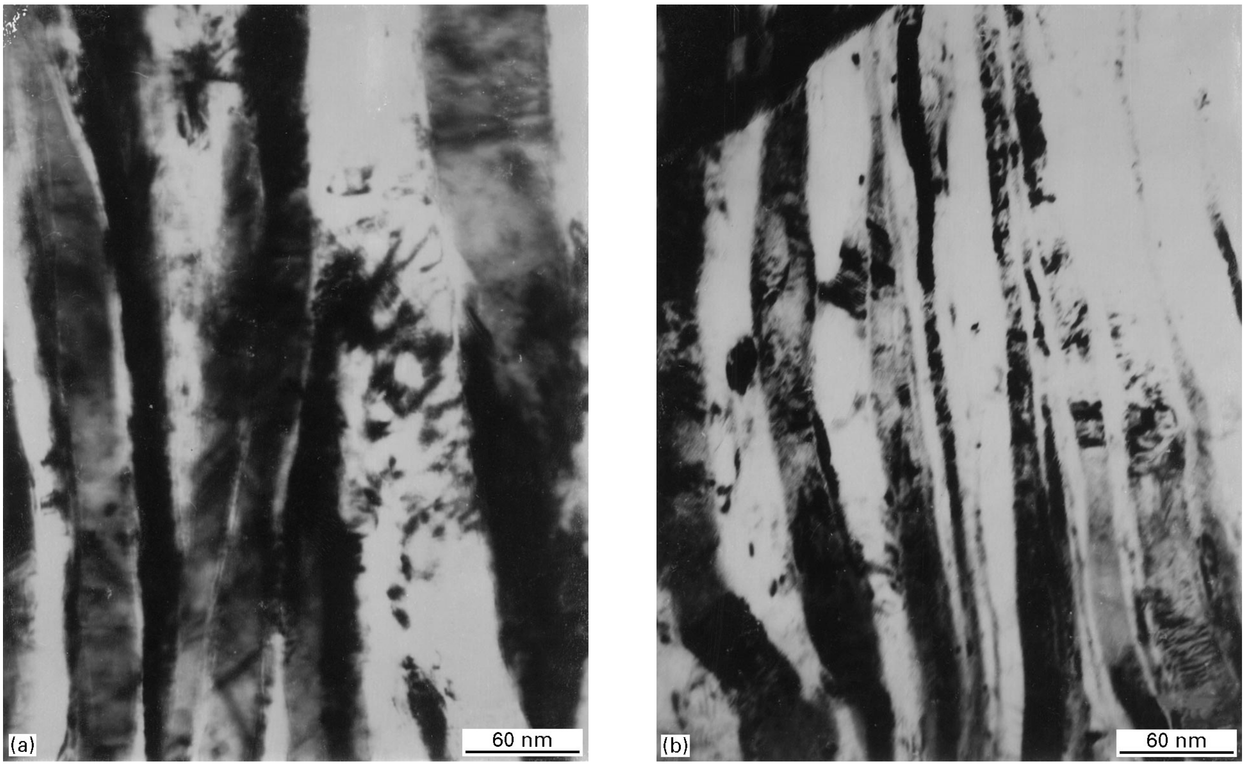

*Figure 10* Bright-field transmission electron micrographs of (a) 25 at% Al–75 at% Fe milled for 1 h and (b) 50 at% Al–50 at% Fe milled for 2 h.

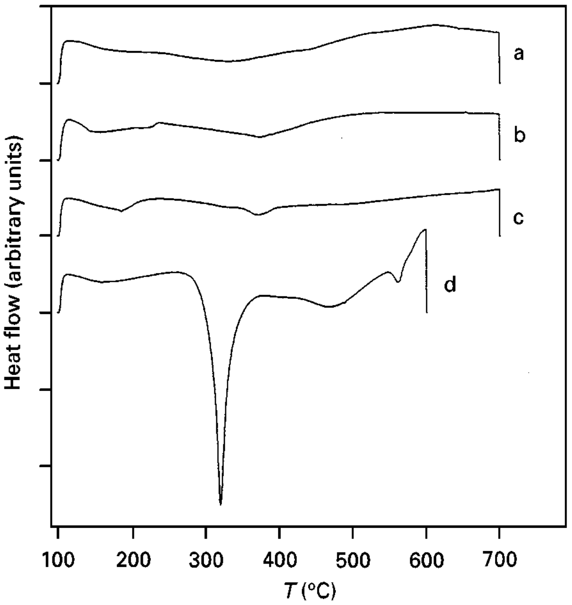

*Figure 11* DSC thermograms of (a) 25 at% Al–75 at% Fe milled for 5 h, (b) 50 at% Al–50 at% Fe milled for 10 h, (c) 75 at% Al–25 at% Fe milled for 20 h, and (d) 80 at% Al–20 at% Fe milled for 50 h.

Mössbauer spectra show that, both for this and for the Fe-rich composition, heating to 700 °C is not sufficient for homogenization of samples pre-milled for short or intermediate times, thus stressing the importance of a local probe for revealing structural details due to local disorder.

Contrary to the above results, the formation of the Fe(Al) solid solution is not observed at the 75 and 80 at% Al compositions, even for milling times sufficiently short that the parent elemental phases have not yet been entirely consumed. The parameters of the non-magnetic phase which develops during milling are close to those of the $Al_5Fe_2$ compound, thus showing that the prevailing mechanism operating in these samples is diffusion of Fe into Al.

Further evidence relative to the asymmetry in the diffusion rates of Al and Fe has been obtained by EDS microanalysis which shows that the concentration of Al into Fe is lower than the concentration of Fe into Al for both the Fe-rich and the equiatomic compositions.

## 5. Conclusions

In conclusion, the results obtained by Mössbauer spectroscopy and by EDS microanalysis show that during high-energy ball milling of samples containing 50 or 75 at% Fe there is diffusion of both elements into each other with an indication that at least in the early stages of milling the concentration of Fe into Al grows at a faster rate than the concentration of Al into Fe. This feature is exhibited to an even greater extent by the Al-rich samples where the only reaction detected by Mössbauer spectroscopy is the formation of a non-magnetic phase whose composition and local coordination is similar to $Al_5Fe_2$. A final remark concerns the 75 and 80 at% Al samples whose different behaviour with respect to ball milling and heat treatment have already been reported [4]. Milling of the 75 at% Al–25 at% Fe samples leads to the nucleation of the $Al_5Fe_2$ phase which is the only phase detected by XRD after milling for a sufficient time or after heating to 400 °C. Milling of the 80 at% Al–20 at% Fe samples, in contrast, leads to the formation of an ultrafine-grained phase with coherent domains of $d \approx 1$–$2$ nm whose structure is very difficult to define on the basis of XRD or electron diffraction, but which appears to have a local coordination similar to $Al_5Fe_2$ according to Mössbauer spectroscopy. This phase is observed in the XRD patterns of samples heated to 430 °C but transforms to the $Al_3Fe$ phase after heating to 700 °C. All these transformations are observed in the corresponding Mössbauer spectra, thus confirming that, as discussed in [4], the nucleation of $Al_3Fe$ proceeds always through the transformation of an intermetallic compound and that neither ball milling nor heat treatment is able to induce its nucleation from the elemental powders.

## Acknowledgements

We thank M. Vittori Antisari for many useful discussions. We acknowledge the assistance of M. Federici, R. Marazzi and F. Pierdominici for helping with the experimental part. One of us (R.G.) acknowledges a fellowship grant by the International Centre for Theoretical Physics, Tzieste, Italy.

The work has been partially funded by Consiglio Nazionale delle Ricerche and Ministero dell' Università e della Ricerca Scientifica e Tecnologica.

## References

1. C. C. KOCH, in "Materials science and technology. A comprehensive treatment", Vol. 15, edited by R. W. Cahn (VCH, Weinheim, 1991) p. 193.
2. F. CARDELLINI, G. MAZZONE, A. MONTONE and M. VITTORI ANTISARI, *Acta Metall. Mater.* **42** (1994) 2445.
3. F. CARDELLLINI, V. CONTINI and G. MAZZONE, *J. Mater. Sci.* **31** (1996) 4175.
4. F. CARDELLLINI, V. CONTINI, G. MAZZONE and A. MONTONE, *Phil. Mag.* **B76** (1997) 629.
5. G. MAZZONE and M. VITTORI ANTISARI, *Phys. Rev. B* **54** (1996) 441.
6. C. SURYANARAYANA, *Int. Mater. Rev.* **40** (1995) 41.
7. S. ENZO, R. FRATTINI, R. GUPTA, P. P. MACRÌ, G. PRINCIPI, L. SCHIFFINI and G. SCIPIONE, *Acta Mater.* **44** (1996) 3105.
8. D. K. MUKHOPADHYAY, C. SURYANARAYANA and F. H. FROES, *Metall. Trans. A* **26** (1995) 1939.
9. E. BONETTI, S. ENZO, G. PRINCIPI and L. SCHIFFINI, in: "Processing and properties of nanocrystalline materials", edited by C. Suryanarayana, J. Singh and F. H. Froes (Metallurgical Society of AIME, Warrendale, PA, 1996) p. 153.
10. F. CARDELLINI, G. MAZZONE and M. VITTORI ANTISARI, *Acta Mater.* **44** (1996) 1511.
11. J. TANG, W. ZHAO, L. LI, A. U. FALSTER, W. B. SIMMONS Jr, W. L. ZHOU, Y. IKUHARA and J. H. ZHANG, *J. Mater. Res.* **11** (1996) 733.
12. B. L. HUANG, R. J. PEREZ, E. J. LAVERNIA and M. J. LUTON, *NanoStruct. Mater.* **7** (1996) 67.
13. S. NASU, U. GOMER and R. S. PRESTON, *J. Physique, Colloque C1, Supplement* 1 **41** (1980) C1-385.
14. Z. Q. GAO and B. FULTZ, *Phil. Mag. B* **67** (1993) 787.

*Received 11 September 1997*
*and accepted 5 February 1998*